A New Concept for a Low-Dose Stationary Tomographic Molecular Breast Imaging Camera Using 3D Position Sensitive CZT Detectors

Alexander Cherlin, *Member, IEEE,* Andras Wirth, Kjell Erlandsson, Ian Baistow, Kris Thielemans, *Senior Member, IEEE,* Brian F Hutton, *Senior Member, IEEE*

Abstract–**Pixelated CZT detectors have been used in a variety of molecular imaging applications for many years. The interplay of gamma camera and collimator geometric design, gantry motion, and image reconstruction determines the image quality and dose-time-FOV trade-offs. In particular, Molecular Breast Imaging (MBI) has been shown to provide excellent diagnostic results in patients with dense breast tissue, but higher than mammography patient dose and long imaging time impede its wide adoption. We propose a new transformative system concept combining the advantages of CZT detectors (superior energy and position resolution and depth of interaction sensing), multi-pinhole collimation and novel image reconstruction to mitigate those drawbacks without compromising diagnostic content. The closely spaced pinholes allow tomographic image reconstruction, improve sensitivity and angular sampling, but result in significant multiplexing. Novel de-multiplexing algorithms have been developed to mitigate the adverse multiplexing artefacts using the DOI. GATE simulations of the new camera demonstrate a potential to reduce the patient dose by at least a factor of 5 in comparison to planar MBI, thus reducing the dose to the level of an average mammography scan. The first prototype has been built at Kromek with 3D position sensitive CZT detectors and is being evaluated using an "activity-painting" setup with a point ^{57}Co source. Initial results demonstrate the expected performance improvement with the use of sub-pixelisation and DOI. The next steps of the development will include accurate evaluation of the image quality and the dose reduction followed by building a larger scale clinical prototype using optimised detector design.**

I. INTRODUCTION

MAMMOGRAPHY is a widely used screening technique for breast cancer detection, but its sensitivity is strongly reduced in patients with dense breasts tissue. Molecular breast imaging (MBI) using a pair of planar detector arrays has been shown to deliver much better sensitivity in this patient cohort [1,2]. However, long imaging time and radiation dose that is higher than mammography impede its widespread adoption in clinical practice. Several tomographic MBI systems have been proposed involving complex mechanics [3], dual modality systems, slit-slat collimators [4], and more [5]. Simpler dual head systems with non-multiplexing multi-pinhole (MPH) collimators [6] have also been designed, but they require rotation or motion to cover the required field-of-view (FOV). Our goal was to design a stationary tomographic system for complementary breast screening, with the associated effective dose similar to an average mammogram scan and imaging time of within twice that of mammography.

II. METHODS

The new design concept is based on utilising tomographic imaging to improve the contrast of the reconstructed image. The required angular sampling is achieved by the use of two opposing camera heads with MPH collimators comprised of a large number of closely spaced pinholes (Fig.1). The large number of pinholes is essential to achieve the necessary angular sampling without motion and to increase the efficiency of utilising the injected gamma radiation to reduce the effective patient dose. The MPH collimators are positioned close to the high spatial resolution CZT detectors. The acquired data have significant multiplexing (overlap of projections from adjacent pinholes) which leads to artefacts due to ambiguity in the origin of emitted photons. Proprietary de-multiplexing image reconstruction algorithms were developed to reduce the adverse effects of the artefacts using the high-resolution 3D position capabilities of CZT detectors [7].

The new camera design and one of the existing parallel hole collimation systems have been implemented in GATE simulation models [8]. The simulations allowed us to evaluate the feasibility of the proposed design, to compare its performance with the planar MBI, and to support the de-multiplexing algorithm development. The simulation results were used to design and build a small proof-of-principle prototype with an assembly of four CZT detector modules with DOI capabilities.

A. Cherlin is with Kromek Ltd, Sedgefield, County Durham, TS21 3FD, UK (e-mail: alex.cherlin@kromek.com).

A. Wirth is with Kromek Ltd, Sedgefield, County Durham, TS21 3FD, UK (e-mail: andrew.wirth@kromek.com).

I. Baistow is with Kromek Ltd, Sedgefield, County Durham, TS21 3FD, UK (e-mail: ian.baistow@kromek.com).

K. Erlandsson is with the Institute of Nuclear Medicine, University College London, NW1 2BU, UK (e-mail: k.erlandsson@ucl.ac.uk).

K. Thielemans is with the Institute of Nuclear Medicine, University College London, NW1 2BU, UK (e-mail: k.thielemans@ucl.ac.uk).

B.H. Hutton is with the Institute of Nuclear Medicine, University College London, NW1 2BU, UK (e-mail: b.hutton@ucl.ac.uk).

A. Simulated Detector Design & De-Multiplexing Requirements

Basing on initial detector performance requirements, a 6x8 array comprised of 7.3 mm thick CZT detectors with 2 mm pixels was simulated. The results demonstrated that 2x2 sub-pixelisation (equivalent to 1 mm virtual pixels) and at least three DOI layers would allow effective de-multiplexing in the image reconstruction. The configuration of the tungsten MPH collimators with square apertures was optimised for 5 mm lesion detection and 2 min acquisition time (comparing to the average 10 min acquisition time with planar MBI). The optimal performance was achieved with short detector-collimator distances of ~3 mm, aperture diameter of ~2 mm, opening angle of ~90° and inter-aperture spacing of ~10 mm. More detailed review of the optimisation process and de-multiplexing image reconstruction could be found in [7,9].

B. Proof-of-Principle Prototype Performance

The detector prototype was designed and built based on the existing Kromek's DMatrix gamma imager. It was comprised of four (in 2x2 array) 7.3 mm thick CZT detectors with 11x11 array of 2 mm pixels. The detectors were operated at 1000V. The average energy resolution (FWHM) of all four modules was measured as 2.0% or 2.4 keV at 122 keV. The required 2x2 sub-pixelisation of 2 mm pixels has been achieved and implemented in the image reconstruction process. The depth resolution was estimated around the middle of the detector using a 300 µm tungsten collimator. The FWHM was estimated as ~1.2 mm.

C. Phantom "Activity-Painting"

The imaging performance of the prototype is characterised with a small 3D printed tungsten MPH collimator mounted on a positioning jig. The 3D phantoms are emulated using a 3-axis motorised stage assembly and a point ^{57}Co source, following the methodology described in [10]. The stages provide continuous movement of the source in space at a variable speed, thus creating an imprint of a 3D activity distribution. The image performance evaluation is currently under way.

III. RESULTS

Fig. 2 demonstrates the results of the GATE simulated comparison of lesion detection efficiency between a parallel hole CZT LumaGEM scanner and our proposed design. The comparison is based on the experimental results reported by Mayo clinic in [11]. The paper describes characterisation of two commercially available MBI scanners – CZT-based LumaGEM and NaI-based Dilon 6800. The imaging performance was evaluated using a contrast phantom (shown in Fig.2) which consists of a series of cylindrical holes of different depth and diameter made in the acrylic base. The holes represent lesions of difference size and activity. The phantom has a 3 mm deep background layer at the midplane. The experimental result reported by Mayo clinic in for the CZT system is shown on top of our simulation results in the plot, and one can see that they are very close. Their measurements were conducted with the scan time of 10 min, which reflects the current clinical practice. Our system demonstrates a slow decrease in the lesion detection efficiency (based on the Rose criterion), going from 44 lesions out of 48 for a 10 min scan down to 40 lesions for a 2.5 min scan. The results are significantly better than the 37 and 23 lesions correspondingly obtained with our LumaGEM simulations.

Fig.3 shows one of the first experimental results with an "activity-printed" phantom comprised of an array of point sources. The results demonstrate that the sub-2 mm-pixel position resolution is essential for reconstructing a meaningful image. Addition of DOI also provides a clear benefit to both axial and transaxial images.

Fig.4 shows a reconstructed image of a 3D phantom comprised of three layers of point sources. The phantom occupied a volume of 45x45x45 mm^3, with 14 mm distance between the source positions. The phantom was "activity-printed" using a 30 uCi (1.1 MBq) 1 mm diameter point ^{57}Co source, with 40 sec acquisition time per point, without additional background activity. The final images were produced with 50 ML-EM iterations. The spatial resolution (FWHM) in the top and bottom planes is 1.67 mm in lateral direction and 2.38 mm in depth. In the middle plane, the resolution is 2.92 and 5.75 mm correspondingly. The lateral resolution is better than depth resolution due to increased angular sampling in the lateral direction. The inferior resolution in the middle slice is due to the lower magnification of the MPH collimation at a bigger distance from the collimator.

IV. DISCUSSION

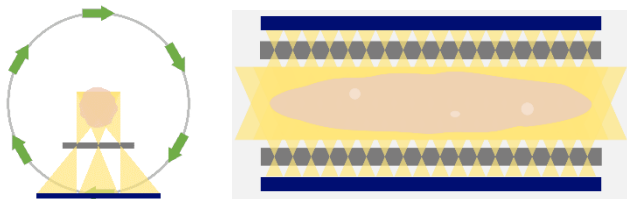The MPH collimation with minimisation of multiplexing

Fig. 1: Conventional multi-pinhole tomographic system concept with a rotating gantry (left); new proposed design with two stationary detector arrays and two multi-pinhole collimators (right).
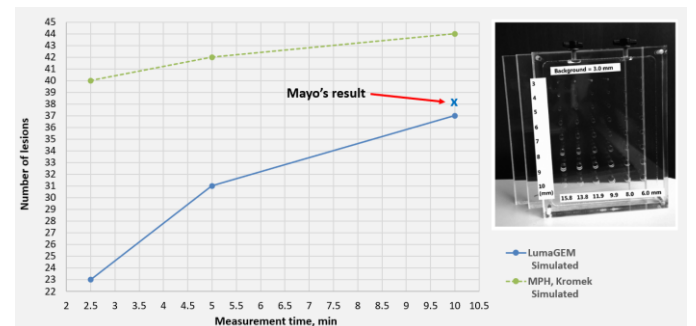

Fig. 2: Left - comparison of lesion detection efficiency in GATE simulations with 48 lesion Mayo clinic's contrast phantom [11] vs. scan time for a parallel hole system (LumaGEM) and Kromek's MPH system. The "X" on the plot shows the experimental result from the paper, obtained in a 10 min scan which is a typical MBI scan time in the clinical practice. Right – Mayo clinic's contrast phantom.
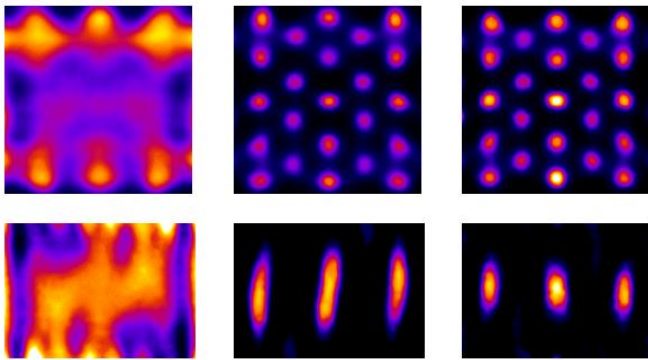
Fig. 3: First measured results of an "activity-printed" phantom comprised of an array of point sources. Top row – image in the detector plane; bottom row – image in the plane perpendicular to the detectors. Columns going from left to right: no sub-pixelisation, no DOI; with sub-pixelisation, no DOI; with sub-pixelisation and DOI.

has been used to improve the image contrast in many systems. We have introduced the new approach to allow a high degree of multiplexing and to use the DOI information provided by CZT detectors for de-multiplexing the data to minimise the image artefacts. The combination of the better image contrast from tomographic images and larger detector sensitivity will allow decreasing the combination of the effective patient dose and the scan time by at least a factor of 5. Such a significant improvement would overcome the main impediments in the MBI adoption and will position our Low-Dose MBI technology on par with the mammography dose for complementary screening of patients with dense breast tissue.

The resulting image quality is affected by the different structure of the image background noise, which is no longer a uniform Poisson noise as in 2D parallel hole imaging. Additional image artefacts are produced by periodic detector features such as detector boundaries. Those factors are being studied using the proof-of-principle prototype. The simulation studies suggest a possibility of additional reduction in the dose and/or screening time. The simulation and experimental results will be combined in the course of the next few months in the design of the next generation prototype of the Low-Dose MBI camera.

REFERENCES

[1] D. J. Rhodes, C. B. Hruska, A. L. Conners, C. L. Tortorelli, R. W. Maxwell, K. N. Jones, A. Y. Toledano, M. K. O'Connor, "Molecular breast imaging at reduced radiation dose for supplemental screening in mammographically dense breasts", AJR Am J Roentgenol, vol. 204, no. 2, pp. 241-251, Feb. 2015.
[2] C. B. Hruska, "Molecular breast imaging for screening in dense breasts: state of the art and future directions", AJR Am J Roentgenol, vol. 208, no. 2, pp. 275-283, Feb. 2017.
[3] J. P. Shah, S. D. Mann, R. L. McKinley, M. P. Tornai, "Implementation and CT sampling characterization of a third-generation SPECT-CT system for dedicated breast imaging", J. of Medical Imaging, vol. 4, no. 3, p. 033502, Jul. 2017.
[4] J. van Roosmalen, F. J. Beekman, M. C. Goorden, "Comparison of fan-beam, slit-slat and multi-pinhole collimators for molecular breast tomosynthesis", Phys. Med. Biol., vol. 63, no. 10, pp. 105009-105020, May 2018.
[5] J. J. James, S. L. Tennant, "Contrast-enhanced spectral mammography (CESM)", Clin. Radiol., vol. 73, no. 8, pp. 715-723, Aug. 2018.
[6] J. van Roosmalen, M. C. Goorden, F. J. Beekman, "Molecular breast tomosynthesis with scanning focus multi-pinhole cameras", Phys. Med. Biol., vol. 61, no. 15, pp. 5508-28, Jul. 2016.
[7] B. F. Hutton, K. Erlandsson, A. Wirth, I. Baistow, K. Thielemans, A. Cherlin, "Design of an ultra-low-dose, stationary, tomographic Molecular Breast Imaging system", Proc IEEE NSS/MIC 2021.
[8] S. Jan et al., "GATE: a simulation toolkit for PET and SPECT," Phys. Med. Biol., vol. 49, no. 19, pp. 4543-4561, Oct. 2004.
[9] K. Erlandsson, A. Wirth, K. Thielemans, I. Baistow, A. Cherlin, B. F. Hutton, "Challenges in optimization of a stationary tomographic molecular breast imaging system", Proc IEEE NSS/MIC 2021.
[10] A. Forgacs, P. Kallos-Balogh, F. Nagy, A. K. Krizsan, I. Garai, L. Tron, "Activity painting: PET images of freely defined activity distributions applying a novel phantom technique", PLoS ONE., vol. 14, no. 1, e0207658, Jan. 2019.
[11] Z. Long, A. L. Conners, K. N. Hunt, C. B. Hruska, M. K. O'Connor, "Performance characteristics of dedicated molecular breast imaging systems at low doses", Med. Phys., vol. 43, no. 6, pp. 3063-3070, May 2016.
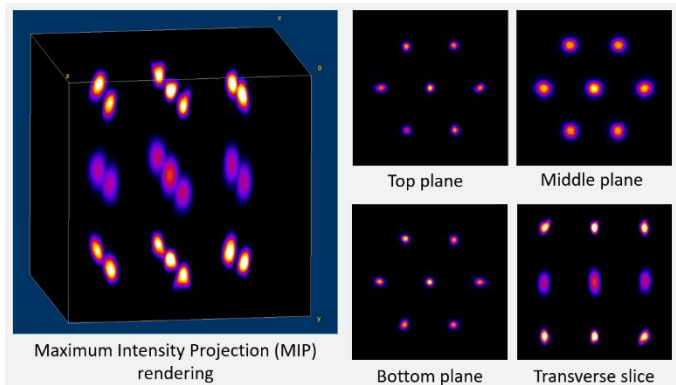
Fig. 4. Reconstructed image of am "activity-printed" 3D phantom comprised of 3 layers of point sources without background activity.